IEEJ Journal of Industry Applications
Vol.7 No.1 pp.93–101 DOI: 10.1541/ieejjia.7.93
Translated from IEEJ Transactions on Industry Applications, Vol.137 No.6 pp.469–477

Paper
(Translation of IEEJ Trans. IA)

Perfect Tracking Control Method by Multirate Feedforward and State Trajectory Generation based on Time Axis Reversal

Wataru Ohnishi* Student Member, Hiroshi Fujimoto* Senior Member

A plant with unstable zeros is known as difficult to control because of initial undershoot of step response and unstable poles of its inversion system. There are two reasons why a plant has unstable zeros in a discrete time domain: 1) non collocation of actuators and sensors and 2) discretization by zero-order hold. Problem 2) has been solved using the perfect tracking control (PTC) method based on multirate feedforward control proposed by our research group. However, the conventional PTC method cannot achieve the perfect tracking for a plant with continuous-time unstable zeros because of the divergence of the desired state trajectories. This paper proposes a preactuation perfect tracking control (PPTC) method to solve problem 1) through the state trajectory generation based on a time axis reversal. The validity of the proposed method is demonstrated through simulations in comparison with three single-rate feedforward control methods.

Keywords: time axis reversal, multirate feedforward, unstable intrinsic zeros, unstable discretization zeros

1. Introduction

The roots of the denominator polynomial of the transfer function are known as poles and the roots of the numerator polynomial are called zeros. If the poles and zeros lie in the right half plane (RHP) in the case of a continuous time system, or are located outside the unit circle in the case of a discrete time system, they are known as unstable poles and zeros, respectively. A plant with unstable zeros gives rise to an initial undershoot when stepped as shown in Fig. 1 [1], and further, the inverse system for feedforward control has unstable poles. Therefore, such a plant is difficult to control. The zeros in the discrete time system are classified as follows: 1) intrinsic zeros that correspond to the zeros of the continuous time system [2][3] and 2) the discretization zeros [4].

When the zeros of the continuous time system are unstable, the intrinsic zeros become unstable. The zeros of the continuous time system are determined by the matrices $\boldsymbol{A}$, $\boldsymbol{b}$, $\boldsymbol{c}$ in the state space representation of the plant. In other words, besides the dynamics of the plant, the position and characteristic of the sensors and the actuators also have a role in determining the zeros [5]. Some examples of plants having unstable zeros in continuous time domain are: the wafer stage of a semiconductor exposure apparatus [6], the hard disk drive (HDD) [7], boost converter [8], the permanent magnet synchronous motor during six-step operation [9] and so on. In these cases, the unstable intrinsic zeros are generated by discretization. On the other hand, even when there is no unstable zero in the continuous time transfer function, the discretization zero is unstable when the relative degree is greater than two [4]. Therefore, the inverse system of the plant becomes unstable and perfect tracking cannot be achieved with the single-rate system framework [10].

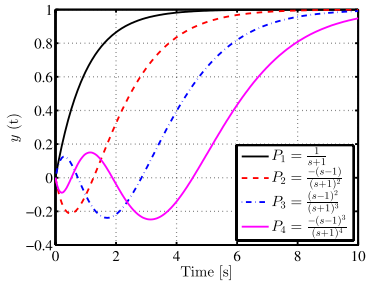

Fig. 1. Step response comparison. P_1 is a first-order transfer function without an unstable zero. P_2, P_3, and P_4 have one, two, and three unstable zero(s), respectively. Step responses of the system with unstable zero(s) creates undershoot

Several methods based on the approximated inverse system have been proposed for designing a stable feedforward (FF) controller when the intrinsic and/or discretization zeros are unstable. For example, the nonminimum-phase zeros ignore (NPZI) method [11], the zero-phase-error tracking control (ZPETC) method [10], and the zero-magnitude-error tracking control (ZMETC) method [12] are proposed. It is noted that since these methods are designed in a discrete time system, the problems of unstable intrinsic and discretization zeros are being dealt with in same time.

Therefore, we have proposed the Perfect Tracking Control (PTC) method [13] using multirate feedforward, which is a method of designing a stable inverse system without approximating to the unstable discretization zeros. This method is applied to high-precision stages [14][15], HDD [7], Atomic Force Microscope (AFM) [16], machine tools [17], etc. However, even in this method, the state variable trajectories are divergent when there are unstable zeros in the continuous time system and hence it becomes necessary to perform an

* Graduate School of Engineering, The University of Tokyo
5-1-5, Kashiwanoha, Kashiwa 277-8561, Japan

approximation [7].

To address this problem, exact inversion methods by preactuation and preview have been proposed [18][19]. Here, preactuation means a change in the feedforward control input before the reference arrives and preview means preknowledge of a future reference trajectory. However, these methods also attempt to deal with unstable intrinsic and discretization zeroes in same time. Continuous-time domain approach has been also proposed [20]. This method solves the differential equation consisting of the plant model and the reference trajectory in continuous time while ignoring discretization zeros.

In this paper, we propose the Preactuation Perfect Tracking Control (PPTC) method which is a stable inversion for unstable intrinsic and discretization zeros without approximation. Stable inversion for unstable intrinsic zeros is performed by state variable trajectory generation by time axis reversal and imaginary axis flipping. The proposed method can be applied to any reference trajectory as long as the $(n-1)$th derivative of the reference trajectory is given (where n denotes the order of the nominal plant). Next, stable inversion for unstable discretization zeros is performed by the multirate feedforward control [13].

In this paper, simulation is performed using the model of an experimental stage in which actuators and sensors are arranged redundantly for rigid body mode. In this stage, the height of the thrust point/measurement point can be changed using the internal and external divisions. As a result, it is possible to change the placement of zeros of the 2nd/5th order transfer function in a continuous time system. Four cases of simulation have been carried out in this paper. Case 1 is the case where there are no zeros. In Case 2, there is one stable zero, Case 3 has one real stable zero and one real unstable zero, and Case 4 is the case having one real unstable zero. In the perfect tracking control method using the conventional multirate feedforward [13], perfect tracking is possible only in the cases where there was no unstable zero in the continuous time system (Case 1, 2). Whereas, in the proposed method with the extended state variable trajectory generation, it is demonstrated that perfect tracking is possible even in cases having continuous time unstable zeros (Case 3, 4).

The simulation of the four types of zero placement described above clarifies the following relationships. 1) Placement of plant zeros in the continuous time system, 2) generation of the state variable trajectory for the perfect tracking of the reference, and 3) preactuation and postactuation control input. Here, postactuation is defined as changing the control input after the reference settling.

2. Single Rate Feedforward Control Method using Approximated Inverse System

In this section, we introduce the NPZI method [11], the ZPETC method [10], and the ZMETC method [12] which are methods for the design of the approximated inverse system of the discrete time domain. A block diagram using the approximated feedforward inverse system is shown in Fig. 2 and the comparison of the three methods is shown in Table 1. Here, it is assumed that, with respect to the sampling period T_y and the control period T_u, $T_y = T_u$, and $z_s = e^{T_u s}$.

If the nominal model $P_n[z_s]$ of the plant discretized by the zero-order hold has unstable zero(s), the pole(s) of the inverse system $P_n^{-1}[z_s]$ for the feedforward controller becomes unstable. We therefore consider designing the approximate inverse system $\tilde{P}_n^{-1}[z_s]$. Let us consider decomposing the zeros into the stable part $B_s[z_s]$ and the unstable part $B_u[z_s]$ as shown in equation (1). Here, equation (1) is irreducible.

$$P_n[z_s] = \frac{B[z_s]}{A[z_s]} = \frac{B_s[z_s]B_u[z_s]}{A[z_s]} \cdots\cdots\cdots\cdots\cdots\cdots (1)$$

$$B_u[z_s] = b_{un_u} z_s^{n_u} + b_{u(n_u-1)} z_s^{n_u-1} + \cdots + b_{u0} \cdots\cdots\cdots (2)$$

Here, n_u is the order of $B_u[z_s]$. Hence, in three methods, the FF controller is designed by using the approximate inverse system $\tilde{P}^{-1}[z_s]$ of $P[z_s]$ as in equation (3). The differences of three methods are design of $B_u^*[z_s]$ and $q(0 \le q \in \mathbb{Z})$.

$$C_{ff}[z_s] = \tilde{P}_n^{-1}[z_s] = \frac{z^{-q}A[z_s]}{B_s[z_s]B_u^*[z_s]} \cdots\cdots\cdots\cdots\cdots (3)$$

2.1 NPZI Method Among the three methods, NPZI method has the least computational cost.

In the NPZI method, $B_u^*[z_s]$ is designed to compensate only the DC term, as shown in equation (4). Here, q is the relative degree of $A[z_s]$ and $B_s[z_s]$.

$$B_{u:Ign}^*[z_s] = B_u[z_s]|_{z_s=1} = B_u[1] \cdots\cdots\cdots\cdots\cdots (4)$$

2.2 ZPETC Method The NPZI method does not take into account the dynamics of the $B_u[z_s]$, while the ZPETC method is designed to have zero phase error as shown in equation (5).

$$B_{u:ZP}^*[z_s] = \frac{(B_u[z_s]|_{z_s=1})^2}{B_u^f[z_s]} = \frac{(B_u[1])^2}{B_u^f[z_s]} \cdots\cdots\cdots\cdots (5)$$

Here, $B_u^f[z_s]$ is defined as in equation (6).

$$B_u^f[z_s] = b_{u0} z_s^{n_u} + b_{u1} z_s^{n_u-1} + \cdots + b_{un_u} \cdots\cdots\cdots\cdots (6)$$

The degree and the coefficient in equation (6) have been flipped from equation (2). By this operation, the unstable zeros located outside the unit circle are projected into the unit circle and made into stable zeros. As shown in Table 1, $C_{ff:\,ZP}[z_s] = C_{ff:\,Ign}\frac{B_{u[z_s]}^f}{Bu[1]}$, which is obtained by adding a phase correction term to the NPZI method transfer function. Here, q is the relative degree of $A[z_s]B_u^f[z_s]$ and $B_s[z_s]$.

By previewing q samples for the reference trajectory and substituting $z_s = exp(j\omega T_u)$ yields Equation (7) [22].

$$\mathrm{Im}\left\{\frac{y[k]}{r[k+q]}\right\} = \mathrm{Im}\left\{\frac{B_u(e^{-j\omega T_s})B_u(e^{j\omega T_s})}{(B_u[1])^2}\right\} = 0$$
$$0 \le \omega \le \pi/T_u \cdots\cdots (7)$$

Thus, it is seen that the phase error is 0 on the entire frequency range up to the Nyquist frequency.

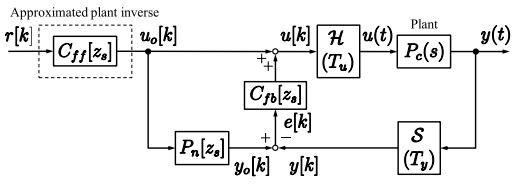

Fig. 2. Approximated plant inverse feedforward control configuration ($C_{ff}[z_s] = \tilde{P}_n^{-1}[z_s]$). $\mathcal{H}$ and $\mathcal{S}$ denote a holder and a sampler, respectively

Table 1. Comparison between NPZI, ZPETC, and ZMETC [11]. $Y[z_s]$ and $R[z_s]$ denote $\mathcal{Z}$ transformed signal of $y(t)$ and $r(t)$ shown in Fig. 2 with sampling time T_u

Method	$C_{ff}[z_s]$	$\frac{Y[z_s]}{R[z_s]}$	Note
NPZI	$C_{ff:Ign}[z_s] = \frac{z_s^{-q}A[z_s]}{B_s[z_s]B_u[1]}$	$\frac{z_s^{-q}B_u[z_s]}{B_u[1]}$	low computation cost
ZPETC	$C_{ff:ZP}[z_s] = \frac{z_s^{-q}A[z_s]B_u^f[z_s]}{B_s[z_s](B_u[1])^2}$	$\frac{z_s^{-q}B_u[z_s]B_u^f[z_s]}{(B_u[1])^2}$	$\mathrm{Im}\left(z_s^q \frac{Y[z_s]}{R[z_s]}\right) = 0$ (zero phase error)
ZMETC	$C_{ff:ZM}[z_s] = \frac{z_s^{-q}A[z_s]}{B_s[z_s]B_u^f[z_s]}$	$\frac{z_s^{-q}B_u[z_s]}{B_u^f[z_s]}$	$\left\lvert\frac{Y[z_s]}{R[z_s]}\right\rvert = 1$ (zero magnitude error)

2.3 ZMETC Method In the ZMETC method, the unstable zero is converted into a stable pole of the approximated inverse system by equation (8).

$$B^*_{u:ZM}[z_s] = B^f_u[z_s] \cdots\cdots (8)$$

Here, q is the relative degree of $A[z_s]$, and $B_s[z_s]B^f_u[z_s]$. In the ZMETC method, there is no gain error on the entire frequency domain, as shown in Table 1.

3. FF Control Method for a Plant with Continuous Time Unstable Zeros (Preactuation Perfect Tracking Control Method)

The perfect tracking control method based on the multirate feedforward shown in Fig. 3 [13] is a technique to design a stable inverse system for unstable discretization zeros. However, even in this method, since the state variable trajectory diverges when there are unstable zeros in the continuous time system, it is necessary to perform approximation in the continuous time system [7]. In this paper, we resolve this problem by generating a state variable trajectory using time axis reversal as shown in section 3.2, and propose a method by which to achieve perfect tracking even for a plant with continuous time unstable zeros.

3.1 Definition The nominal plant in the continuous time system is defined in equation (9). Here, $P_c(s)$ is irreducible.

$$\begin{cases} P_c(s) = \dfrac{B(s)}{A(s)} = \dfrac{b_m s^m + b_{m-1}s^{m-1} + \cdots + b_0}{s^n + a_{n-1}s^{n-1}\cdots + a_0} \\ A(s) = \dfrac{s^n + a_{n-1}s^{n-1}\cdots + a_0}{b_0} \\ B(s) = \dfrac{b_m s^m + b_{m-1}s^{m-1} + \cdots + b_0}{b_0} \end{cases} \cdots\cdots (9)$$

Equation (10) is state space realization of equation (9) by the controllable canonical form shown in equation (11).

$$\dot{\boldsymbol{x}}(t) = \boldsymbol{A}_c\boldsymbol{x}(t) + \boldsymbol{b}_c u(t),\ y(t) = \boldsymbol{c}_c\boldsymbol{x}(t) \cdots\cdots (10)$$

$$\begin{cases} \boldsymbol{x} = \begin{bmatrix} x_1 \\ x_2 \\ \vdots \\ x_n \end{bmatrix}, \boldsymbol{A}_c = \begin{bmatrix} 0 & 1 & 0 & \cdots & 0 \\ 0 & 0 & 1 & \cdots & 0 \\ & & & \ddots & \\ -a_0 & -a_1 & -a_2 & \cdots & -a_{n-1} \end{bmatrix} \\ \boldsymbol{b}_c = \begin{bmatrix} 0 & 0 & \cdots & b_0 \end{bmatrix}^{\mathrm{T}} \\ \boldsymbol{c}_c = \begin{bmatrix} 1 & \frac{b_1}{b_0} & \cdots & \frac{b_m}{b_0} & 0 & \cdots & 0 \end{bmatrix} \end{cases} \cdots\cdots (11)$$

Here, n and m ($< n$) represent the order of $A(s)$ and $B(s)$, respectively. The continuous time state equation shown in the equation (10) is discretized with the sampling period T_u to obtain equation (12).

$$\boldsymbol{x}[k+1] = \boldsymbol{A}_s\boldsymbol{x}[k] + \boldsymbol{b}_s u[k],\ y[k] = \boldsymbol{c}_s\boldsymbol{x}[k] \cdots\cdots (12)$$

Here, $\boldsymbol{A}_s$, $\boldsymbol{b}_s$, $\boldsymbol{c}_s$ are obtained using equation (13).

$$\boldsymbol{A}_s = e^{\boldsymbol{A}_c T_u},\ \boldsymbol{b}_s = \int_0^{T_u} e^{\boldsymbol{A}_c\tau}\boldsymbol{b}_c d\tau,\ \boldsymbol{c}_s = \boldsymbol{c}_c \cdots\cdots (13)$$

3.2 State Variable Trajectory $x_d(t)$ Generation In order for the output $y(t)$ to track the reference trajectory $r(t)$, the state variable trajectory $\boldsymbol{x}_d(t)$ needs to satisfy equation (14), as seen from equation (10).

$$r(t) = \boldsymbol{c}_c\boldsymbol{x}_d(t) \cdots\cdots (14)$$

Further, the differential values of the reference trajectory are assumed to be given as in equation (15).

$$\begin{aligned} \boldsymbol{r}(t) &= \begin{bmatrix} r_1(t) & r_2(t) & \cdots & r_n(t) \end{bmatrix}^{\mathrm{T}} \\ &= \begin{bmatrix} 1 & \frac{d}{dt} & \cdots & \frac{d^{n-1}}{dt^{n-1}} \end{bmatrix}^{\mathrm{T}} r(t) \end{aligned} \cdots\cdots (15)$$

Next, we generate the state variable trajectory $\boldsymbol{x}_d(t)$ from $\boldsymbol{r}(t)$ using the controllable canonical realization of $\boldsymbol{x}_d(t)$. Here, when the plant has unstable zeros, the state variable trajectory diverges. Therefore, we separately generate the stable and unstable part state variable trajectories using the following procedure. The unstable part state trajectory is stably generated by time axis reversal in time domain and imaginary axis reversal in frequency domain.

3.2.1 Stable-unstable Decomposition $B(s)^{-1}$ is decomposed into $F^{st}(s)$ with stable poles and $F^{ust}(s)$ with unstable poles.

$$B(s)^{-1} = F^{\mathrm{st}}(s) + F^{\mathrm{ust}}(s) \cdots\cdots (16)$$

For example, i) $F^{st}(s) = 1$, $F^{ust}(s) = 0$ when $P_c(s)$ does not have zeros, ii) $F^{st}(s) = B(s)^{-1}$, $F^{ust}(s) = 0$ when $P_c(s)$ has only stable zeros, and iii) $F^{st}(s) = 0$ and $F^{ust}(s) = B(s)^{-1}$ when $P_c(s)$ has only unstable zeros. Further, $\bar{\mathcal{L}}$ is defined as a one-sided Laplace transform, and $f^{st}(t)$ and $\bar{f}^{st}(t)$ are defined as in equation (17). It is noted that $F^{ust}(-s)$ is stable and l denotes the number of unstable zeros.

$$f^{\mathrm{st}}(t) = \bar{\mathcal{L}}^{-1}\left[F^{\mathrm{st}}(s)\right], \bar{f}^{\mathrm{ust}}(t) = \bar{\mathcal{L}}^{-1}\left[(-1)^l F^{\mathrm{ust}}(-s)\right] \cdots\cdots (17)$$

3.2.2 Stable Part State Variable Trajectory Generation The stable part state variable trajectory $\boldsymbol{x}^{st}_d(t)$ is generated by equation (18)†.

† Equation (18) can be calculated by analytical convolution (e.g. by using MATLAB Symbolic Math Toolbox). It can be well approximated by filtering operation (e.g. by using MATLAB's lsim command or discrete-time transfer function).

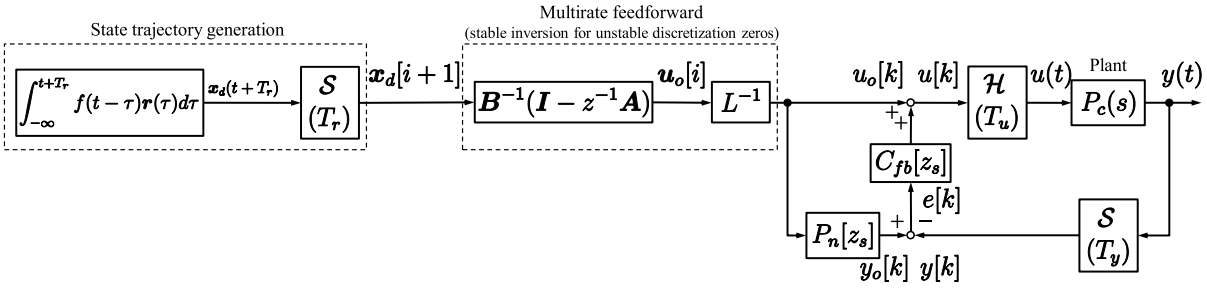

Fig. 3. Perfect Tracking Control method based on multirate feedforward proposed in Ref. (13). $\mathcal{S}$, $\mathcal{H}$, and L denote a sampler, holder, and lifting operator [21], respectively. z and z_s denote e^{sT_r} and e^{sT_u}, respectively

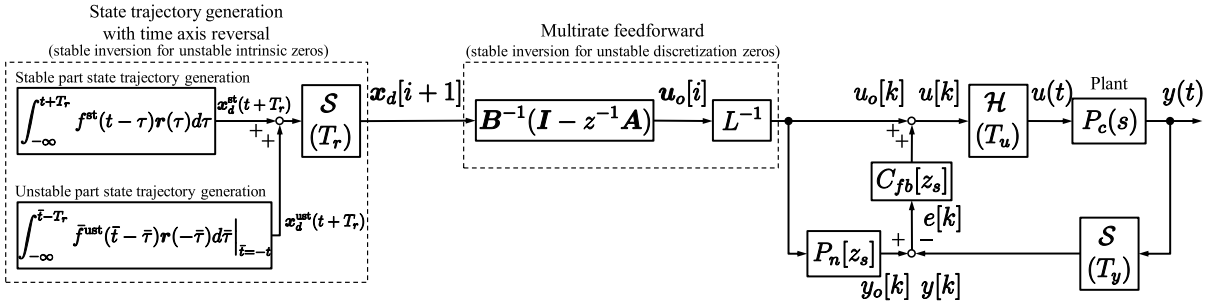

Fig. 4. Proposed Preactuation Perfect Tracking Control method based on multirate feedforward and state trajectory generation by time axis reversal

$$\boldsymbol{x}_d^{\mathrm{st}}(t) = \left[x_{1d}^{\mathrm{st}}(t) \quad x_{2d}^{\mathrm{st}}(t) \quad \cdots \quad x_{nd}^{\mathrm{st}}(t)\right]^{\mathrm{T}} = \int_{-\infty}^{t} f^{\mathrm{st}}(t-\tau)\boldsymbol{r}(\tau)d\tau \cdots\cdots (18)$$

3.2.3 Unstable Part State Variable Trajectory Generation The unstable part state variable trajectory $\boldsymbol{x}_d^{ust}(t)$ is obtained by calculating the convolution of the time axis reversed reference trajectory $\boldsymbol{r}(-\bar{t})$ with the stable signal $\bar{f}^{ust}(\bar{t}-\bar{\tau})$ and further performing time axis reversal on it†. Please refer to Refs. (23), (24) for the proof by bilateral Laplace transform.

$$\boldsymbol{x}_d^{\mathrm{ust}}(t) = \left[x_{1d}^{\mathrm{ust}}(t) \quad x_{2d}^{\mathrm{ust}}(t) \quad \cdots \quad x_{nd}^{\mathrm{ust}}(t)\right]^{\mathrm{T}} = \int_{-\infty}^{\bar{t}} \bar{f}^{\mathrm{ust}}(\bar{t}-\bar{\tau})\boldsymbol{r}(-\bar{\tau})d\bar{\tau}\Big|_{\bar{t}=-t} \cdots\cdots (19)$$

3.2.4 State Variable Trajectory Generation

The state variable trajectory $\boldsymbol{x}_d(t)$ is the sum of the stable and unstable state variable trajectories.

$$\boldsymbol{x}_d(t) = \boldsymbol{x}_d^{\mathrm{st}}(t) + \boldsymbol{x}_d^{\mathrm{ust}}(t) \cdots\cdots (20)$$

3.3 Feedforward Control Input u_o Generation The problem of unstable discretization zeros is resolved by the multirate feedforward control method [13]. We consider the three periods as shown in Fig. 4. T_y and T_r represent the sampling period for the output $y(t)$ and the reference trajectory $r(t)$, and T_u represents the hold period for the control input $u(t)$. In this paper, we set $T_r = nT_u = nT_y$.

The multirate system of equation (12) is given as

$$\boldsymbol{x}[i+1] = \boldsymbol{A}\boldsymbol{x}[i] + \boldsymbol{B}\boldsymbol{u}[i], \quad y[i] = \boldsymbol{c}\boldsymbol{x}[i] \cdots\cdots (21)$$

where

$$\boldsymbol{A} = \boldsymbol{A}_s^n, \quad \boldsymbol{B} = \left[\boldsymbol{A}_s^{n-1}\boldsymbol{b}_s \quad \boldsymbol{A}_s^{n-2}\boldsymbol{b}_s \quad \cdots \quad \boldsymbol{A}_s\boldsymbol{b}_s \quad \boldsymbol{b}_s\right]$$
$$\boldsymbol{c} = \boldsymbol{c}_c, \quad \boldsymbol{x}[i] = \boldsymbol{x}(iT_r) \cdots\cdots (22)$$

Equation (21) is obtained by calculating the state transitions from $t = iT_r = kT_u$ to $t = (i+1)T_r = (k+n)T_u$. The feedforward input $\boldsymbol{u}_o[i]$ is defined by the lifting form shown in equation (23).

$$\boldsymbol{u}_o[i] = \left[u_1[i] \quad u_2[i] \quad \cdots \quad u_n[i]\right]^{\mathrm{T}} = \left[u(kT_u) \quad u((k+1)T_u) \quad \cdots \quad u((k+n-1)T_u)\right]^{\mathrm{T}} \cdots\cdots (23)$$

L in Fig. 4 is the discrete time lifting operator [21]. The input of L^{-1} is n dimensional vector $\boldsymbol{u}_o\,[i]$ with the sampling period T_r. Then the output of L^{-1} is sequential output from $u_1\,[i]$ to $u_n\,[i]$ with the sampling period $T_u = T_r/n$.

Equations (21) and (22) indicate that matrix $\boldsymbol{B}$ is nonsingular in the case of a controllable plant and hence the feedforward input $\boldsymbol{u}_o\,[i]$ can be obtained using equation (24). It is noted here that the $T_r = nT_u$ previewed state variable trajectory $\boldsymbol{x}_d[i+1]$ is used.

$$\boldsymbol{u}_o[i] = \boldsymbol{B}^{-1}(\boldsymbol{I} - z^{-1}\boldsymbol{A})\boldsymbol{x}_d[i+1] \cdots\cdots (24)$$

Here, z denotes e^{sT_r}.

4. Simulation Example

4.1 Simulation Conditions The simulation model used in this paper is the fine stage with 6 degrees of freedom shown in Figs. 5 and 6 [25]. This stage has redundant actuators and sensors for the rigid body mode in the translational direction, and it is possible to make changes to the position

† In equation (19), the convolution operation may be replaced with a filter operation, as in section 3.2.2. However, as this is a process that requires infinite preview time, in practical terms, the length of the trajectory until the stage stops may be sufficient. Further, if there is sufficient memory, it is easier to calculate formula (19) offline and implement it with a header file.

Table 2. Simulation condition and required preview, preactuation, and postactuation time of proposed method to achieve perfect tracking

	L_{fx}	L_m	F^{st}	F^{ust}	Preview time	Preactuation time	Postactuation time	Note
Case 1	0.010	−0.36	1	0	$5T_u$	0	0	$P_c(s)$ with no zeros. PTC is achieved by a method proposed in [13].
Case 2	−0.025	−0.78	$\frac{140}{s+140}$	0	$5T_u$	0	∞	$P_c(s)$ with one stable zero. PTC is achieved by a method proposed in [13].
Case 3	−0.50	0.0050	$\frac{94}{s+180}$	$\frac{-94}{s-200}$	∞	∞	∞	$P_c(s)$ with one stable zero and one unstable zero.
Case 4	0.13	−0.15	0	$\frac{-140}{s-140}$	∞	∞	0	$P_c(s)$ with one unstable zero.

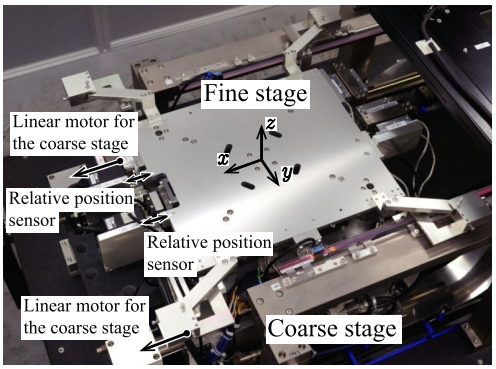

Fig. 5. Photograph of the 6-DOF high-precision stage

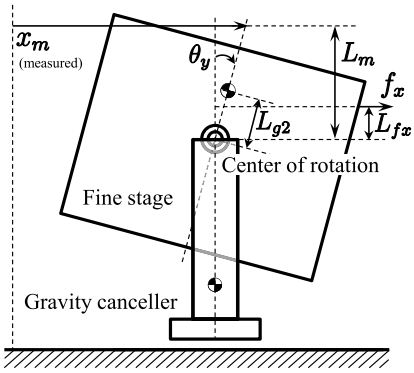

Fig. 6. Fine stage model of the scanning motion x and the pitching motion θ_y [25]

of the thrust point/measurement point by using the internal and external divisions. Therefore, assuming that the height of the thrust point as seen from the center of rotation is L_{fx}, the height of the measurement point is L_m, and the height of the center of gravity point is L_{g2}, as shown in Fig. 6, the transfer function of the continuous time system from the current command signal to the measured position x_m is expressed by equation (25). The current control system is assumed to be a first-order system with poles at $s = -10000$.

$$P_c(s) = \frac{(b_2 s^2 + b_1 s + b_0)}{(s + 1.0\times10^4)(s^2 + 83s + 2100)(s^2 + 25s + 11000)} \quad \cdots\cdots(25)$$

$$\begin{cases} b_2 = 98000(L_{fx} - L_{g2})(L_m - L_{g2}) + 1400 L_{fx} L_m + 1900 \\ b_1 = L_{fx} L_m 8.0\times10^6 + 3.0\times10^4 \\ b_0 = L_{fx} L_m 2.0\times10^8 - 9.6\times10^5 + 2.2\times10^7 \\ L_{g2} = -0.051 \end{cases} \quad \cdots\cdots(26)$$

In equation (25), the placement of zeros changes upon changing the height L_{fx} of the thrust point and L_m of the measurement point. In this paper, we simulate four types of zero placements. Table 2 gives a summary of the simulation conditions. The Bode plots of the four conditions are shown in Fig. 7.

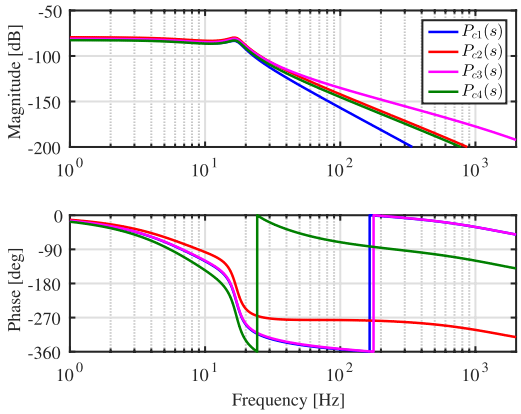

Fig. 7. Bode diagram of the simulation models

The reference trajectory is given by the step trajectory interpolation by a 9th order polynomial as shown in Fig. 8(a). The step time was set to 0.02 seconds. Simulation was carried out with the block diagram shown in Figs. 2 to 4. In this configuration, the feedback controller $C_{fb}[z_s]$ does not work in the absence of modeling error/disturbance. The sampling period was set as $T_u = 100\,\mu$s. In order to simulate the continuous time response, the time step was set to $H = 10\,\mu$s. The simulation was performed in the time interval $-0.5\,\mathrm{s} < \mathrm{t} < 0.5\,\mathrm{s}$. 0.5 seconds is much longer than the time constant of unstable zeros in Case 3 and 4.

Due to space constraints, only the position dimensions $x_{1d}^{\mathrm{st}}(t)$, $x_{1d}^{\mathrm{ust}}(t)$, $x_{1d}(t)$, and the velocity dimensions $x_{2d}^{\mathrm{st}}(t)$, $x_{2d}^{\mathrm{ust}}(t)$, $x_{2d}(t)$ have been shown.

4.2 Simulation Results

4.2.1 Plant with no Zeros (Case 1) Taking $L_{fx} = 0.010$, and $L_m = -0.36$, equation (27) is obtained. Discretized transfer function by zero-order hold is shown in equation (28). The denominator polynomial (29) in discrete-time is common to the all cases (Case 1–4).

$$P_{c1}(s) = \frac{2.2\times10^7}{(s+1.0\times10^4)(s^2+83s+2100)(s^2+25s+11000)} \quad \cdots\cdots(27)$$

$$P_{s1}[z_s] = \frac{1.533\times10^{-15}(z+20.01)(z+1.988)(z+0.3607)(z+0.03557)}{A[z_s]} \quad \cdots\cdots(28)$$

$$A[z_s] = (z-0.3679)(z^2-1.992z+0.9918)(z^2-1.997z+0.9975) \quad \cdots\cdots(29)$$

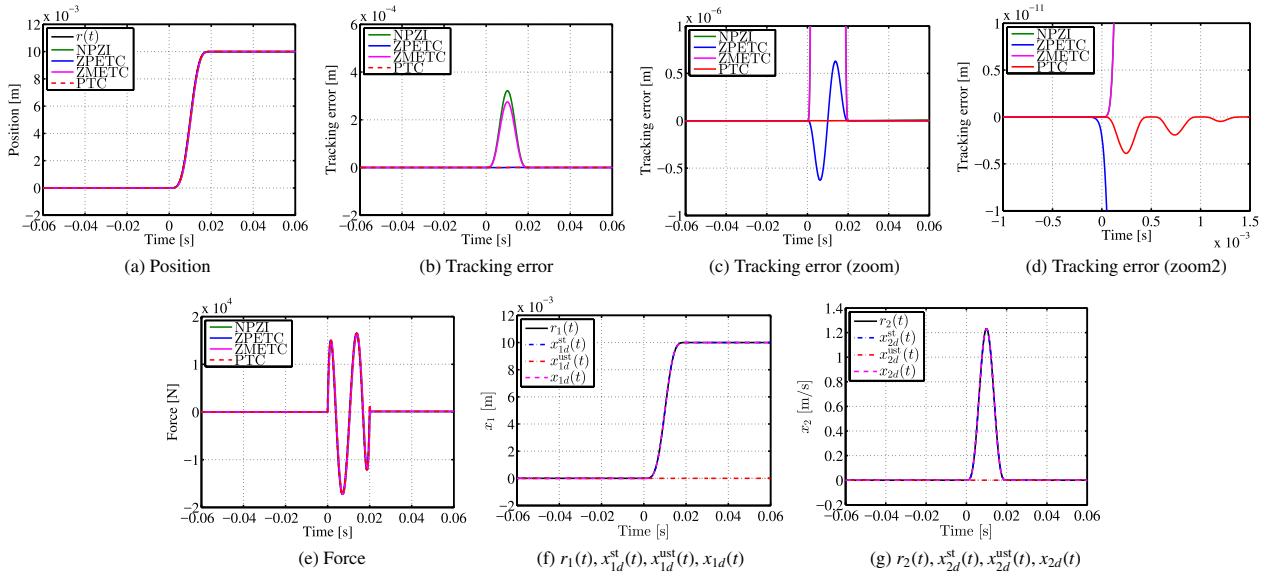

(a) Position (b) Tracking error (c) Tracking error (zoom) (d) Tracking error (zoom2)

(e) Force (f) $r_1(t), x_{1d}^{\mathrm{st}}(t), x_{1d}^{\mathrm{ust}}(t), x_{1d}(t)$ (g) $r_2(t), x_{2d}^{\mathrm{st}}(t), x_{2d}^{\mathrm{ust}}(t), x_{2d}(t)$

Fig. 8. Simulation results of the plant without zeros (Case 1)

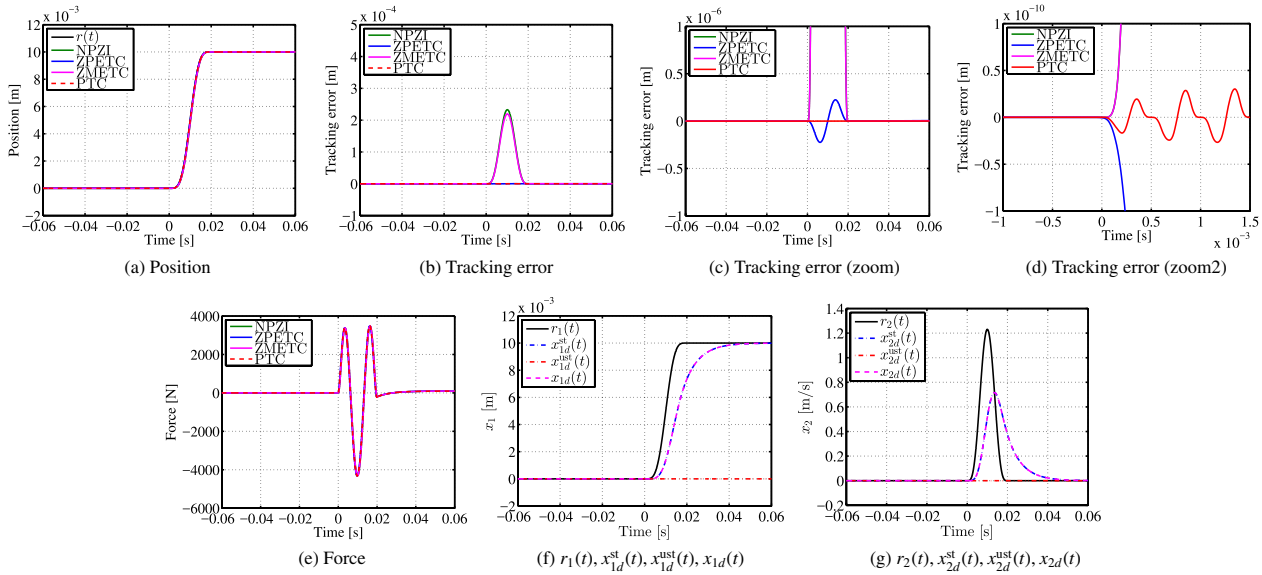

(a) Position (b) Tracking error (c) Tracking error (zoom) (d) Tracking error (zoom2)

(e) Force (f) $r_1(t), x_{1d}^{\mathrm{st}}(t), x_{1d}^{\mathrm{ust}}(t), x_{1d}(t)$ (g) $r_2(t), x_{2d}^{\mathrm{st}}(t), x_{2d}^{\mathrm{ust}}(t), x_{2d}(t)$

Fig. 9. Simulation results of the plant with one stable zero (Case 2)

The simulation results are shown in Fig. 8. It is seen from Figs. 8(b) and (c) that, the three methods NPZI, ZPETC and ZMETC are affected by approximation of the unstable discretization zeros, resulting in tracking errors. Fig. 8(d) shows that, in the PTC method, the tracking error is 0 in every period $T_r = nT_u = 500\,\mu$s, and perfect tracking is achieved. Further, since there are no zeros, it can be seen that the state variable trajectory $\boldsymbol{x}_d(t)$ shown in Figs. 8(f) and 8(g) coincides with the reference values of each dimension.

4.2.2 Plant with a Real Stable Zero (Case 2)

Taking $L_{fx} = -0.025$, and $L_m = -0.78$, equation (30) and (31) are obtained.

$$P_{c2}(s) = \frac{1.9 \times 10^5 (s+140)}{(s+1.0\times10^4)(s^2+83s+2100)(s^2+25s+11000)} \quad \cdots\cdots(30)$$

$$P_{s2}[z_s] = \frac{6.417 \times 10^{-13}(z+8.303)(z+0.8219)(z-0.9859)(z+0.08072)}{A[z_s]} \quad \cdots\cdots(31)$$

The simulation results are shown in Fig. 9. Since there is a stable zero on the real axis in continuous time, as shown in Figs. 9(f) and (g), the state variable trajectory $\boldsymbol{x}_d^{\mathrm{st}}(t)$ is first-order lagged compared with the reference trajectory $\boldsymbol{r}(t)$. As a result, postactuation is performed as shown in Fig. 9(e). Fig. 9(d) shows that, in the PTC method, the error is 0 in every period $T_r = nT_u = 500\,\mu$s, and perfect tracking is achieved.

4.2.3 Plant with a Real Stable Zero and an Unstable Zero (Case 3)

Taking $L_{fx} = -0.050$, and $L_m = -0.0050$, equation (32) and (33) are obtained.

$$P_{c3}(s) = \frac{-620(s-200)(s+180)}{(s+1.0\times10^4)(s^2+83s+2100)(s^2+25s+11000)} \quad \cdots\cdots(32)$$

$$P_{s3}[z_s] = \frac{-8.178 \times 10^{-11}(z+2.962)(z-1.02)(z-0.9822)(z+0.2039)}{A[z_s]} \quad \cdots\cdots(33)$$

The simulation results are shown in Fig. 10. From Figs. 10(f) and (g), it is seen that the state variable trajectory $\boldsymbol{x}_d^{\mathrm{ust}}(t)$ is

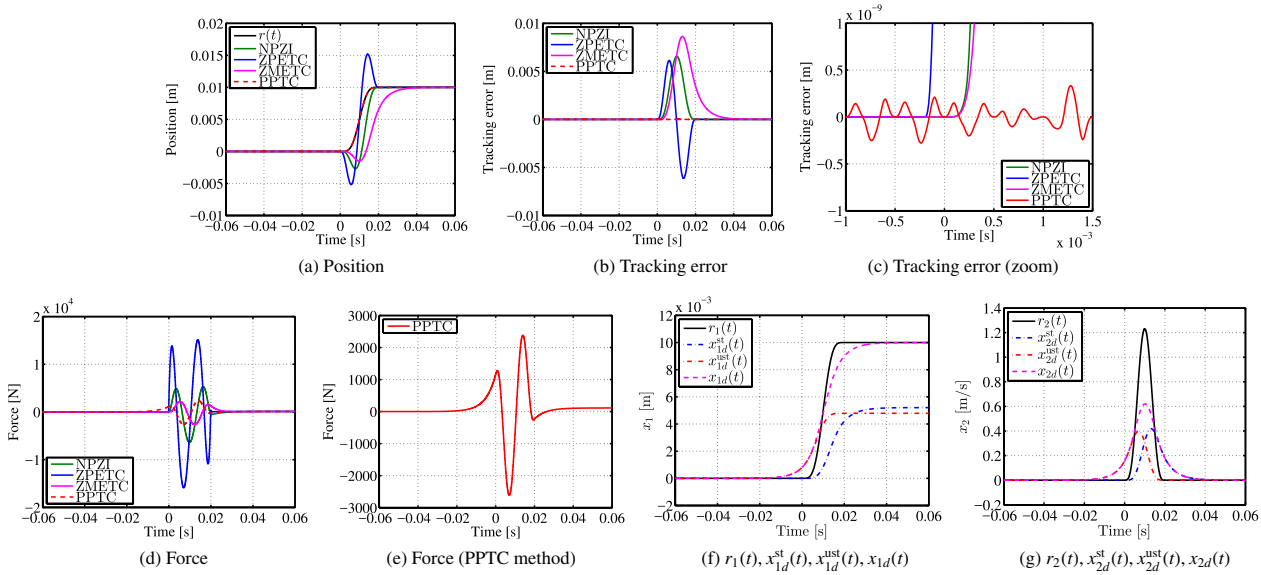

(a) Position (b) Tracking error (c) Tracking error (zoom)

(d) Force (e) Force (PPTC method) (f) $r_1(t), x_{1d}^{st}(t), x_{1d}^{ust}(t), x_{1d}(t)$ (g) $r_2(t), x_{2d}^{st}(t), x_{2d}^{ust}(t), x_{2d}(t)$

Fig. 10. Simulation results of the plant with one stable zero and one unstable zero (Case 3)

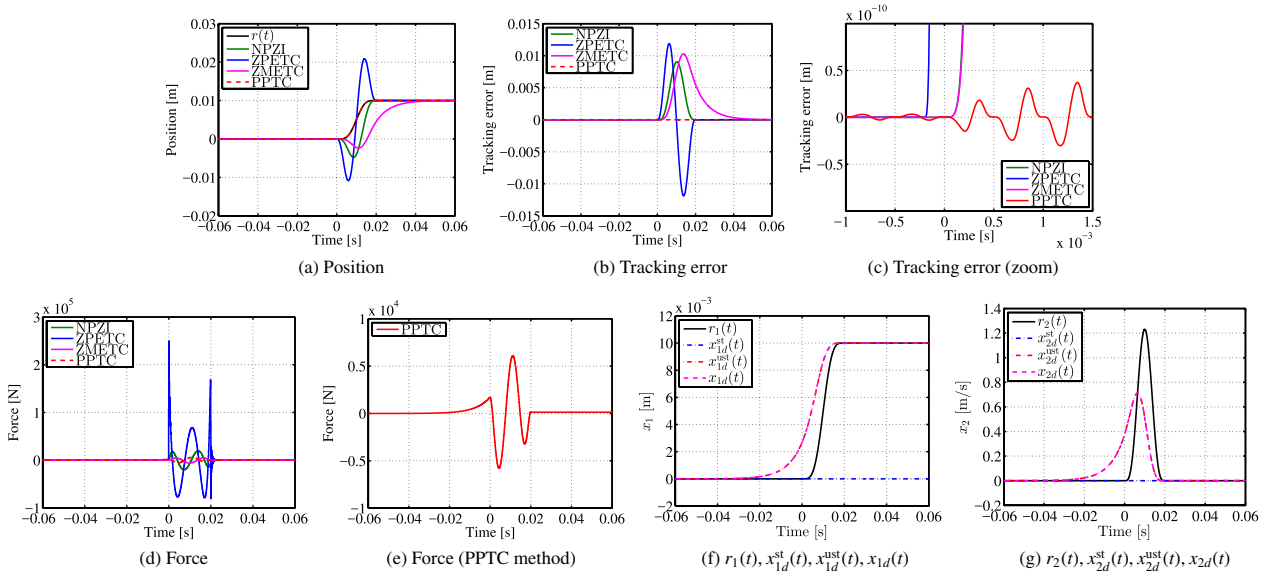

(a) Position (b) Tracking error (c) Tracking error (zoom)

(d) Force (e) Force (PPTC method) (f) $r_1(t), x_{1d}^{st}(t), x_{1d}^{ust}(t), x_{1d}(t)$ (g) $r_2(t), x_{2d}^{st}(t), x_{2d}^{ust}(t), x_{2d}(t)$

Fig. 11. Simulation results of the plant with one unstable zero (Case 4)

generated during $t < 0$ due to the effect of the unstable zero in continuous time domain. Similarly, it changes to $\boldsymbol{x}_d^{st}(t)$ during $0.02s < t$ due to the influence of the stable zero in continuous time domain. As a result of these influences, the feedforward control input with preactuation and postactuation shown in Fig. 10(d) is generated. From Fig. 10(c), it is seen that in the PPTC method, the tracking error is 0 in every period $T_r = nT_u = 500\,\mu$s, not only when $0 < t$ but also when $t < 0$, indicating that perfect tracking has been achieved.

4.2.4 Plant with a Real Unstable Zero (Case 4) Taking $L_{fx} = 0.13$, and $L_m = -0.15$, equation (34) and (35) are obtained.

$$P_{c4}(s) = \frac{-1.299 \times 10^5 (s-140)}{(s+1.0\times10^4)(s^2+83s+2100)(s^2+25s+11000)} \quad \cdots\cdots(34)$$

$$P_{s4}[z_s] = \frac{-4.466 \times 10^{-13}(z+8.253)(z+0.8172)(z-1.014)(z+0.08029)}{A[z_s]} \quad \cdots\cdots(35)$$

The simulation results are shown in Fig. 11. Since the plant has one real unstable zero, the state variable trajectory $\boldsymbol{x}_d^{ust}(t)$ has a nonzero value at $t < 0$, as shown in Figs. 11(f) and (g). Hence, a preactuated feedforward input is generated as shown in Fig. 11(d). On the other hand, since there is no stable zero in continuous time, there is no postactuation. From Fig. 11(c), the tracking error is 0 in every period $T_r = nT_u = 500\,\mu$s in the PPTC method, and perfect tracking has been achieved.

4.2.5 Summary of Simulation Results As described above, in all the Cases 1 to 4, irrespective of the placement of zeros, the tracking error is zero in every period $T_r = nT_u = 500\,\mu$s in the PTC and PPTC methods, showing that perfect tracking has been achieved. In addition, as put forth in Table 2, it has been shown that the following feedforward inputs are necessary to achieve perfect tracking.
(1) Plant with no zeros in the continuous time plant
Neither preactuation nor postactuation is required, and perfect tracking by $T_r = nT_u$ preview.

(2) Plant with stable zeros in the continuous time plant

Infinite time postactuation is required in addition to preview of $T_r = nT_u$.

(3) Plant with unstable zeros in the continuous time plant

Infinite time preactuation is required in addition to infinite time preview.

5. Conclusion

In the discretized domain, there are two types of zeros: 1) the intrinsic zeros which have counterparts in the continuous time domain, 2) the discretization zeros generated by discretization. The problem of designing a stable inverse system for a plant with unstable discretization zeros is resolved by the perfect tracking control (PTC) method using multirate feedforward control [13]. Therefore, in this paper, we have proposed the Preactuation Perfect Tracking Control (PPTC) method, which is an extension of the state variable trajectory generation method. This method enables perfect tracking of control for a plant with unstable zeros in continuous time systems, which was not possible in the conventional PTC method.

Based on the premise that the future reference trajectory is already known, the stable state variable trajectory is obtained by the convolution of the inverse of the imaginary axis reversed unstable zeros and the time axis reversed reference trajectory and further performing time-axis reversal. As a result, the state variable trajectory becomes non-zero even before $t = 0$, when the reference trajectory is applied. Applying multirate feedforward for the obtained state variable trajectory, we get a nonzero feedforward signal in negative time (preactuation). In this paper, using the high-precision stage as an example, we simulated four types of arrangement of zeros in a continuous time system, namely, the case with no zeros, the case with only a stable zero, the case having both stable and unstable zeros, and the case with only unstable zero and showed that perfect tracking is possible in all the cases. When the plant has unstable poles, this can be applied by stabilizing the plant through feedback by configuring the feedforward closed-loop inverse (FFCLI) [18]. Moreover, in the case of plant with input delay, perfect tracking can be done by shifting the reference trajectory (preview).

Although this method requires infinite time preactuation, as shown in the simulation results, practical results can be obtained through preactuation that is sufficiently longer than the time constant of the unstable zeros. Discussion of the trade-off between the preactuation truncation within a short time and the tracking error is a future work.

Generally, mechanical structure is rigorously designed so as not to have unstable zeros to the extent possible. When unstable zeros were inevitable, perfect tracking was abandoned because of the approximated inverse system. We believe that, with the PPTC method, the constraints on the design of the mechanical structure can be relaxed in the applications where preactuation is possible and present new options.

Acknowledgment

This research has been partially aided by JSPS Grant-in-Aid for Scientific Research 15 J 08488.

References

(1) T. Matsuo: "Zeroes and Their Relevance to Control [IV] Relationship between Zeros and Output Responses", Journal of The Society of Instrument and Control Engineers, Vol.29, No.6, pp.543–550 (1990) (in Japanese) https://www.jstage.jst.go.jp/article/sicejl1962/29/6/29_6_543/_article/references/-char/ja/

(2) T. Hagiwara, T. Yuasa, and M. Araki: "Stability of the limiting zeros of sampled-data systems with zero-and first-order holds", *International Journal of Control*, Vol.58, No.6, pp.1325–1346 (1993)

(3) T. Hagiwara: "Analytic study on the intrinsic zeros of sampled-data systems", *IEEE Trans. Automatic Control*, Vol.41, No.2, pp.261–263 (1996)

(4) K. Åström, P. Hagander, and J. Sternby: "Zeros of sampled systems", *Automatica*, Vol.20, No.1, pp.31–38 (1984)

(5) J. Hoagg and D. Bernstein: "Nonminimum-phase zeros - much to do about nothing- classical control - revisited part II", *IEEE Control Systems*, Vol.27, No.3, pp.45–57 (2007)

(6) H. Butler: "Position Control in Lithographic Equipment", *IEEE Control Systems Magazine*, Vol.31, No.5, pp.28–47 (2011)

(7) H. Fujimoto, K. Fukushima, and S. Nakagawa: "Vibration suppression short-span seeking of HDD with multirate feedforward control", in American Control Conference, pp.582–587 (2006)

(8) D. Takei, H. Fujimoto, and Y. Hori: "Load Current Feedforward Control of Boost Converter for Downsizing the Output Filter Capacitor", *IEEJ Trans. IA*, Vol.135 No.5 pp.457–466 (2015) (in Japanese) https://www.jstage.jst.go.jp/article/ieejias/135/5/135_457/_article

(9) T. Miyajima, H. Fujimoto, and M. Fujitsuna: "A Precise Model-Based Design of Voltage Phase Controller for IPMSM", *IEEE Trans. on Power Electronics*, Vol.28, No.12, pp.5655–5664 (2013)

(10) M. Tomizuka: "Zero phase error tracking algorithm for digital control", Journal of Dynamic Systems, Measurement, and Control, Vol.109, pp.65–68 (1987)

(11) J.A. Butterworth, L.Y. Pao, and D.Y. Abramovitch: "Analysis and comparison of three discrete-time feedforward model-inverse control techniques for nonminimum-phase systems", *Mechatronics*, Vol.22, No.5, pp.577–587 (2012)

(12) J. Wen and B. Potsaid: "An experimental study of a high performance motion control system", in American Control Conference, Vol.6, pp.5158–5163 (2004)

(13) H. Fujimoto, Y. Hori, and A. Kawamura: "Perfect tracking control based on multirate feedforward control with generalized sampling periods", *IEEE Trans. on Industrial Electronics*, Vol.48, No.3, pp.636–644 (2001)

(14) K. Saiki, A. Hara, K. Sakata, and H. Fujimoto: "A Study on High-Speed and High-Precision Tracking Control of Large-Scale Stage Using Perfect Tracking Control Method Based on Multirate Feedforward Control", *IEEE Transactions on Industrial Electronics*, Vol.57, No.4, pp.1393–1400 (2010)

(15) H. Fujimoto, K. Sakata, and K. Saiki: "Application of Perfect Tracking Control to Large-Scale High-Precision Stage", in 5th IFAC Symposium on Mechatronic Systems, pp.188–193 (2010)

(16) T. Shiraishi and H. Fujimoto: "Positioning control for Piezo scanner using multirate perfect inverse model based iterative learning control", in IEEE/ASME International Conference on Advanced Intelligent Mechatronics, pp.993–998 (2010)

(17) H. Fujimoto and T. Takemura: "High-precision control of ball-screw-driven stage based on repetitive control using n-times learning filter", *IEEE Transactions on Industrial Electronics*, Vol.61, No.7, pp.3694–3703 (2014)

(18) B. Rigney, L.Y. Pao, and D. Lawrence: "Nonminimum phase dynamic inversion for settle time applications", *IEEE Transactions on Control Systems Technology*, Vol.17, No.5, pp.989–1005 (2009)

(19) L. Marconi, G. Marro, and C. Melchiorri: "A solution technique for almost perfect tracking of non-minimum-phase, discrete-time linear systems", International Journal of Control, Vol.74, No.5, pp.496–506 (2001)

(20) T. Shiraishi and H. Fujimoto: "A Reference Trajectory Generation for System with Unstable Zeros Considering Negative-time Domain Analysis", in IEEJ International Workshop on Sensing, Actuation, and Motion Control (2015)

(21) T. Chen and B.A. Francis, Optimal Sampled-Data Control Systems (1996)

(22) T. Yamaguchi, M. Hirata, and H. Fujimoto: "Nanoscale servo control", Tokyo Denki University Press (2007) (in Japanese) http://ci.nii.ac.jp/ncid/BA83531915

(23) T. Sogo: "Calculation of the Non-causal Solution for the Model-matching Problem and Its Application to Preview Feedforward Control", Transactions of the Society of Instrument and Control Engineers, Vol.42 No.1, pp.40–46 (2006) (in Japanese) https://www.jstage.jst.go.jp/article/sicetr1965/42/1/42_1_40/_article/-char/ja/

(24) T. Sogo: "On the equivalence between stable inversion for nonminimum

phase systems and reciprocal transfer functions defined by the two-sided Laplace transform", *Automatica*, Vol.46, No.1, pp.122–126 (2010)
(25) W. Ohnishi, H. Fujimoto, K. Sakata, K. Suzuki, and K. Saiki: "Decoupling Control Method for High-Precision Stages using Multiple Actuators considering the Misalignment among the Actuation Point, Center of Gravity, and Center of Rotation", *IEEJ Journal of Industry Applications*, Vol.5, No.2, pp.141–147 (2016)

Wataru Ohnishi (Student Member) received the B.S. and M.S. degrees from the University of Tokyo in 2013 and 2015, respectively. He is currently working towards the Ph.D. degree in the Department of Electrical Engineering and Information Systems, the University of Tokyo, Japan. He is also a research fellow (DC1) of Japan Society for the Promotion of Science from 2015. He received the IEEJ Excellent Presentation Award in 2014 and the Dean's Award for Outstanding Achievement from the Graduate School of Frontier Sciences, the University of Tokyo in 2015. His research interest is high-precision motion control. He is a student member of the Institute of Electrical and Electronics Engineers.

Hiroshi Fujimoto (Senior Member) received the Ph.D. degree in the Department of Electrical Engineering from the University of Tokyo in 2001. In 2001, he joined the Department of Electrical Engineering, Nagaoka University of Technology, Niigata, Japan, as a research associate. From 2002 to 2003, he was a visiting scholar in the School of Mechanical Engineering, Purdue University, U.S.A. In 2004, he joined the Department of Electrical and Computer Engineering, Yokohama National University, Yokohama, Japan, as a lecturer and he became an associate professor in 2005. He is currently an associate professor of the University of Tokyo since 2010. He received the Best Paper Award from the IEEE Transactions on Industrial Electronics in 2001 and 2013, Isao Takahashi Power Electronics Award in 2010, Best Author Prize of SICE in 2010, and The Grand Nagamori Award in 2016. His interests are in control engineering, motion control, nano-scale servo systems, electric vehicle control, and motor drive. Dr. Fujimoto is a member of IEEE, the Society of Instrument and Control Engineers, the Robotics Society of Japan, and the Society of Automotive Engineers of Japan.